Drying Shrinkage behaviour of foam – cement panel: A numerical study

Payal Desai
Assistant Professor, School of Science and Engineering,
Navrachana University, Bhayli, Vadodara
Email: payald@nuv.ac.in (corresponding author)

Abstract: Shrinkage is an important contributor to slab movements. It is therefore necessary to include it for a realistic physical modelling of shrinkage. Shrinkage of concrete is modelled by an application of a strain profile across the depth of the slab. Application of shrinkage to the cement sheet is performed in the present work. The 3D numerical modelling of a cement and foam sheet with glass fibre mesh in ABAQUS has been presented. Two numerical examples are studied in the present work. (1) Foam-cement sheet embedded with glass fibre (2) Foam – cement sheet not embedded with glass fibre. Numerical results are obtained for both cases. Maximum principal stresses, displacements and logarithmic strain are obtained.

Keywords: Shrinkage of cement, Foam – Cement Panel, numerical analysis, strain profile

1. Introduction

Drying shrinkage is the result of loss of water due to environment action (evaporation, diffusion) and can lead to slab curling and warping. Shrinkage effects/loads can lead to axial and bending stresses in the slabs. Bending stresses are caused by slab curling, which is a result of the shortening and expansion of the slab in a non-uniform manner across the cross-section (Fig. 1). Since curling occurs concurrently with slab contraction/expansion, slab actions due to shrinkage are accounted in the present work. Drying shrinkage is indeed a highly non-uniform phenomenon. Shrinkage rate increases non-linearly from the bottom to the top of the slab due to greater moisture loss happening on top of the slab [1, 2, and 3]. Kim and Lee [1] suggested an analysis of differential drying shrinkage in concrete in which creep of concrete is considered. The authors recall

that the non-uniform moisture distribution in concrete causes differential drying shrinkage. Tensile stress occurs on the exposed surface of concrete structures and may result in crack formation. It was observed that this residual stress was significantly affected by creep of concrete, essentially in the form of shrinkage-induced stresses. From the results of this investigation on differential drying shrinkage by the authors [1], the following conclusions were drawn: The internal drying shrinkage strain significantly varied according to the depth from drying surface, and the stresses induced by this differential drying shrinkage could cause surface cracks. Thus the differential drying shrinkage must be considered in the analysis of thick concrete structures.

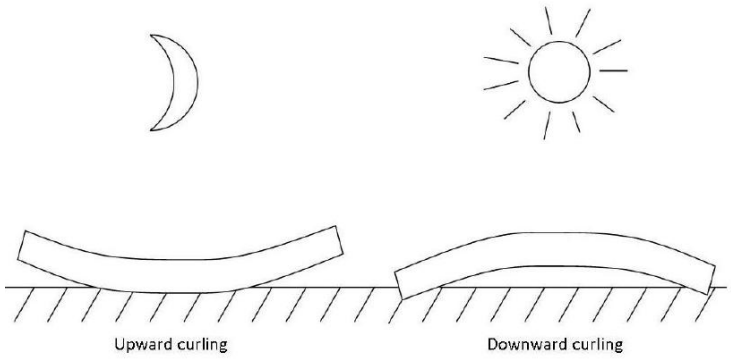

Fig.1 Night – time and day- time slab curling

2. Shrinkage Effects Modelling

As was mentioned previously, shrinkage is an important contributor to slab movements. It is therefore necessary to include it for a realistic physical modelling of shrinkage. Shrinkage of concrete is modelled by an application of a strain profile across the depth of the slab. The review of several models and experimental data shows that the shrinkage strain profiles at a given time are highly nonlinear, and consists of two parts: a constant, low strain at the bottom half of the slab, and an exponential increase of strain from mid-depth to the slab surface. Kim and Lee [1] showed that at any given time, a drastic reduction in shrinkage occurred below a concrete depth of 120 mm. The maximum shrinkage strain in the experimental study by Kim was about 350 micro strains with creep considered. We can note here that this is less than the lower end of the range recommended by ACI- 209 [5] for ultimate shrinkage strain of 415 micro strains, and approximately half of the ultimate shrinkage strain for standard conditions, 780 micro strains.

For the current analysis, an ultimate shrinkage strain of 400 microstrains was assumed as representative of typical shrinkage strain occurring in normal concrete. To implement shrinkage in the model, it was considered that the centre of the slab was submitted to unrestrained shrinkage in the vertical direction; a shrinkage profile depending only on slab height was implemented in ABAQUS using an equivalent temperature distribution. Low shrinkage strains were assigned to the lower half of the concrete slab, and an exponential strain profile is used. Total shrinkage strain can be represented by Eq. (1), a third parameter was added in the equation because it allows modifying the shape of the profile more easily, if ever it was needed to calibrate the shrinkage strain profile [4].

$$\varepsilon_{sh}(y) = a + b.e^{\lambda y} \quad (1)$$

Where ε_{sh} is strain expressed in microstrains, y is slab height in mm and t is time in days.

The conditions were initially assumed for ultimate strains to fit with the shrinkage strain profile derived by Kim and Lee [1]. Figure 2 represents the ultimate shrinkage profile as well as the shrinkage profiles at different times based on ACI-209 [5]; one can observe that the profile after 1 year is almost identical to the ultimate profile.

$$\varepsilon_{sh,u}\ (y = 250) = 400$$

$$\varepsilon_{sh,u}\ (y = 125) = 37.5$$

$$\varepsilon_{sh,u}\ (y = 0) = 25$$

By fitting the three parameters a, b and λ from Eq. (1) to the three values of shrinkage strain above, it comes: a = 24.55, b = 0.4465 and λ = 0.0269.

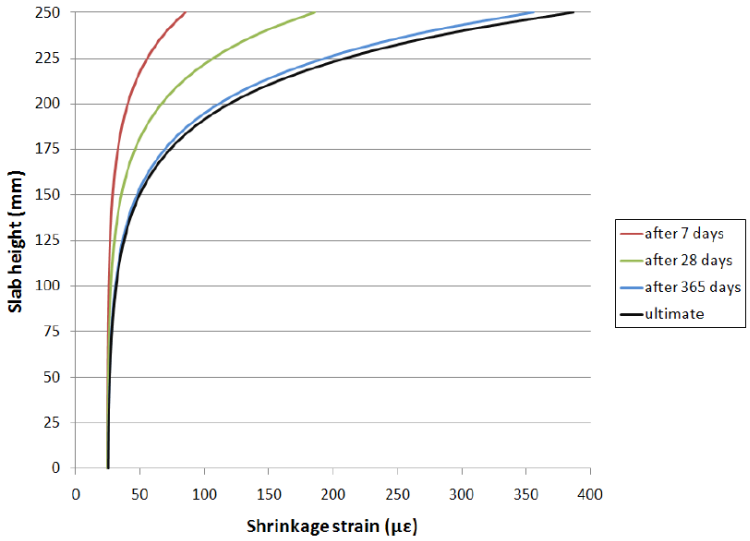

Fig. 2 Variation of shrinkage strain profile across slab depth [5].

In order to simulate the shrinkage strains in the 3D-FEM model, they are treated as thermal strains. Using the relation $\varepsilon sh,u = \alpha c \times Tsh,u$, where $\varepsilon sh,u$ is the ultimate shrinkage strain, αc the coefficient of thermal expansion of concrete and Tsh,u the equivalent temperature variation, the shrinkage strain profile can be converted to a temperature profile (Eq. 2).

$$Tsh(y, t) = (A + B\ e^{\lambda y}) \qquad (2)$$

With A= -2.232, B = -0.04059, λ = 0.0269. The ultimate equivalent temperature gradient between slab top and bottom is then $\Delta(T)$ = -34.1°C, which represents ultimate shrinkage strain condition. Table 1 shows the calculation of temperature through the thickness using Eq. (2)

Table 1 Calculation of temperature gradient through thickness for ultimate strain condition

Sr. No.	Slab Height mm	Delta T in degree C	Slab Height in Inch
1	0	-2.273	0
2	25	-2.312	0.984252
3	50	-2.388	1.9685039
4	75	-2.537	2.9527559
5	100	-2.83	3.9370079
6	125	-3.403	4.9212598
7	150	-4.527	5.9055118
8	175	-6.728	6.8897638
9	200	-11.04	7.8740157
10	225	-19.49	8.8582677
11	250	-36.04	9.8425197

Table 2 Material properties for Cement, Foam and Glass mesh

Property	Glass Mesh	Cement	FLOORMATE 500
Density , ton/mm^3	1.7 x 10^{-9}	2.4 x 10^{-9}	0.04 x 10^{-9}
Young's Modulus, N/mm^2	28000	22500	20
Poisson's Ratio	0.1	0.18	0.001
Coefficient of Linear Thermal Expansion (α_c), 1/°C	4 x 10^{-6}	11x10^{-6}	70x10^{-6}

3. Implementation in ABAQUS

Application of shrinkage to the cement sheet is performed in a single step. The 3D numerical modelling of a cement and foam sheet with glass fibre mesh in ABAQUS has been presented. Fig 3a-3b shows the geometric dimensions and details of the model taken in the present work. Temperature profile calculated in Table 1 is applied through the thickness of the load as predefined temperature field. The material properties for each part of the model are detailed in Table 2. Two numerical examples are studied in the present work. (1) Foam-cement sheet embedded with glass fibre (2) Foam – cement sheet not embedded with glass fibre. 3D stress elements, C3D8R which is an 8 node linear brick elements are used for cement and foam sheets, whereas T3D2 which is a 2 node linear 3-D truss element, is used for glass fibre mesh.

Discussion and Concluding Remarks

Numerical results are obtained for both cases which is shown in Fig. 4a-g and Fig. 5a-d. As expected, because of negative temperature gradient on top of the sheet, upward bending is obtained for the whole model. Maximum principal stresses, displacements and logarithmic strain are shown in Figures. Maximum principal stress in the whole model is 5.63 MPa as shown in Fig. 4a. Displacement variation for glass fibre is shown in Fig. 4b. It is seen that it follows the displacement pattern of cement and foam as shown in Fig. 4c. Maximum central deflection is 0.03 mm, whereas corners of the whole model are lifted by 0.10 mm displacement as shown in Fig. 4c-3d. Maximum principal stress in foam is shown in Fig. 4e. Maximum strain of 364 micron is obtained as in Fig. 4f in cement which is within the limit provided by the ACI code [5]. Fig 4g shows the maximum strain of 1996 micron at 4 tip corners of the foam. This is because of the warpage and curling effect in foam leads to all corners lifted and which is due to the drying shrinkage in cement. There is no much significant improvement is seen in the model without glass fibre embedded in the cement. Deflection is slightly increased from 0.10 mm to 0.11 mm at corners in both cement sheet alone and foam (Fig. 5a-5c). Maximum principal stresses in foam and in whole model are seen in Figs. 5b and 5d respectively. To prevent the corner lift up of foam and cement, corner reinforcement with glass fibre mesh can be provided.

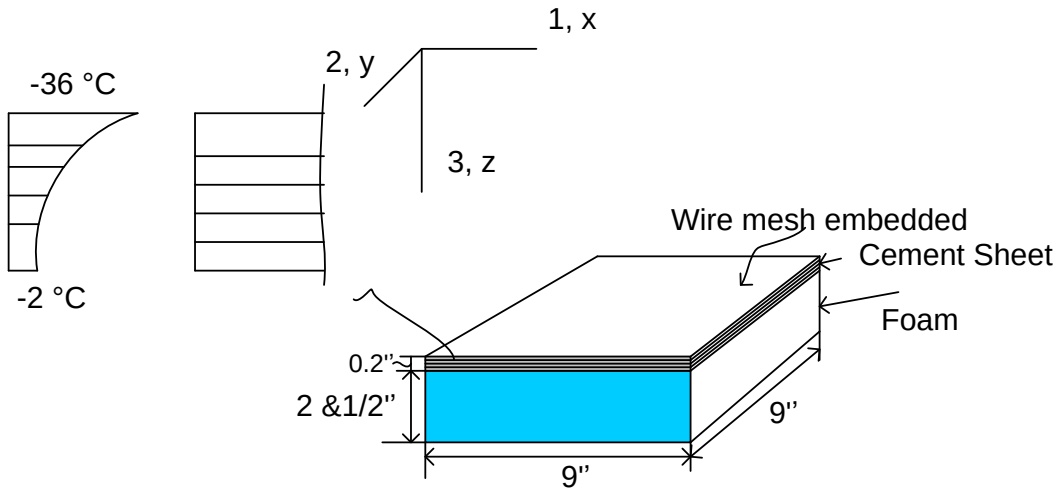

Fig.3a Dimension and details of model

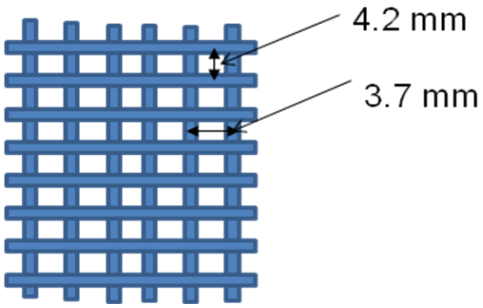

Thickness of strand = 1.0 mm, width of strand = 2.2 mm

Fig. 3b Details of wire mesh

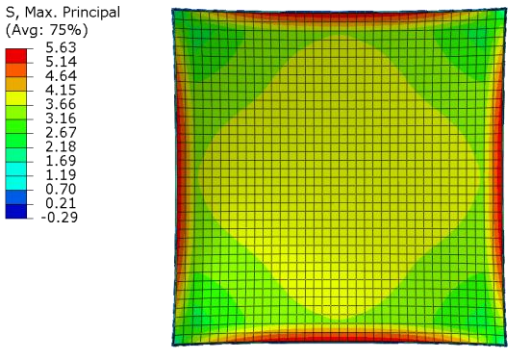

Fig. 4a Maximum principal stresses in the model with glass fibre embedded in cement

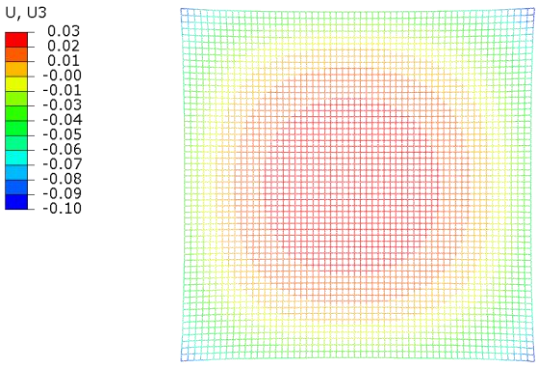

Fig. 4b Maximum displacement in glass fibre embedded in cement

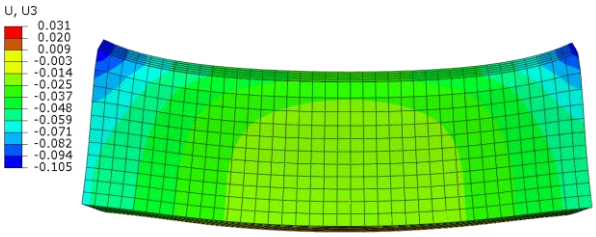

Fig.4c Maximum displacement in the model with glass fibre embedded in cement side view

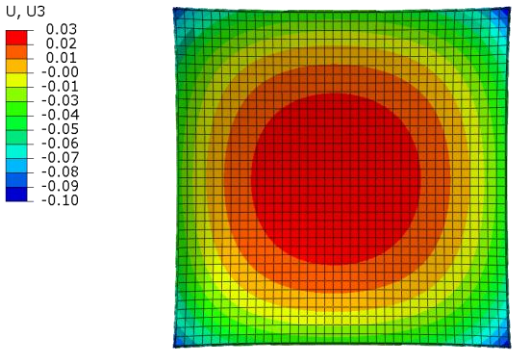

Fig. 4d Maximum displacement in the model with glass fibre embedded in cement top view

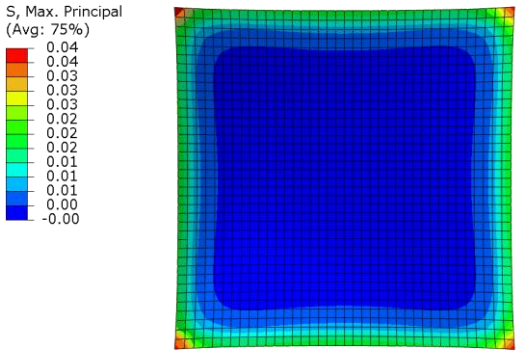

Fig. 4e Maximum principle stress in foam with glass fibre embedded in cement

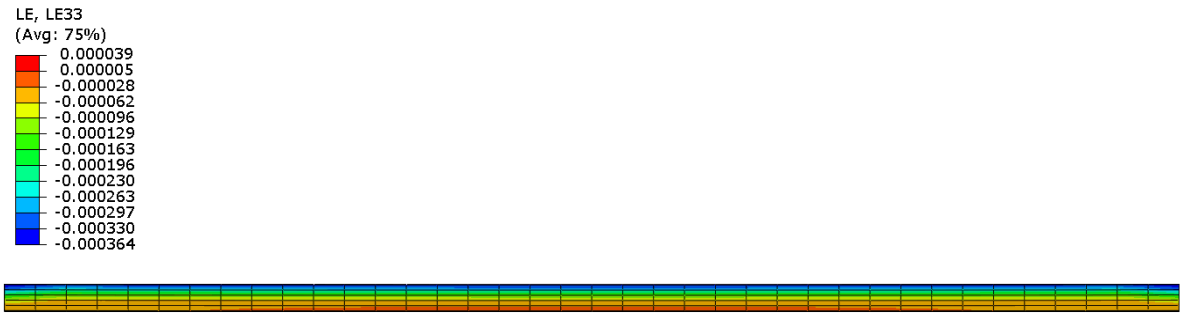

Fig. 4f Maximum logarithmic Strain due to shrinkage in Cement Sheet is 364 microstrain with glass fibre embedded in cement

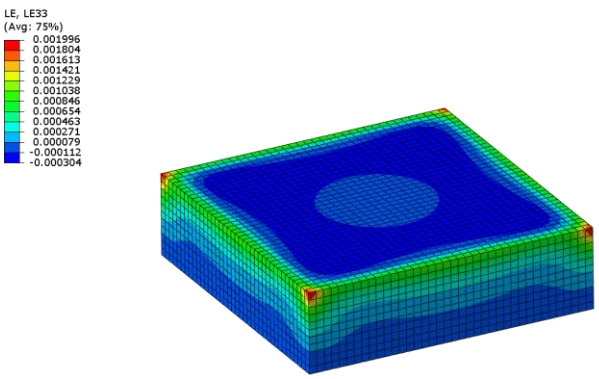

Fig. 4g Maximum logarithmic strain in Foam alone due to shrinkage effect of cement with glass fibre embedded in cement

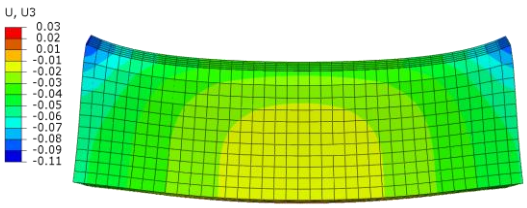

Fig 5a Maximum displacement without glass fibre embedded in cement side view

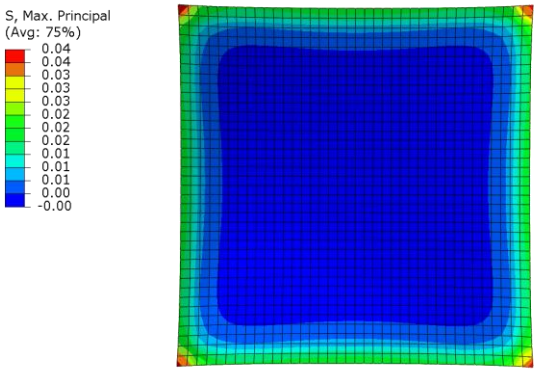

Fig 5b Max principal stress in foam without glass fibre embedded in cement

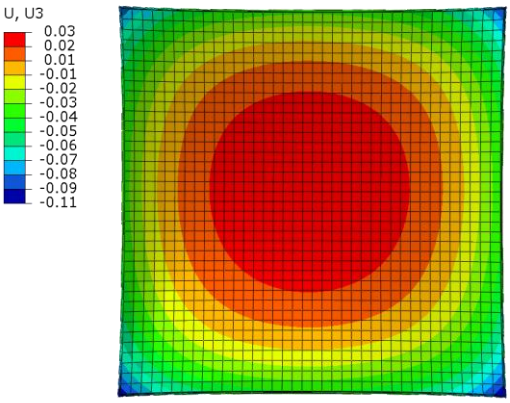

Fig 5c Maximum displacement without glass fibre embedded in cement top view

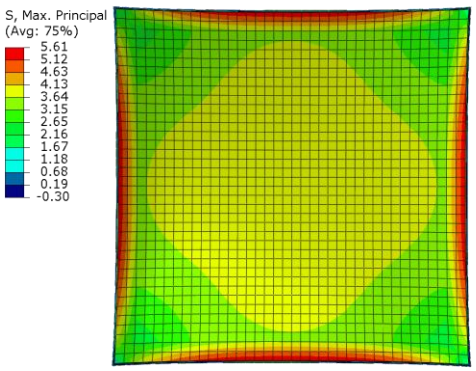

Fig 5d Max principal stress in the model without glass fibre embedded in cement

References

1) Kim, J.-K. and Lee, C.-S. (1998). Prediction of Differential Drying Shrinkage in Concrete. *Cement and Concrete Research*, Vol. 28, No. 7, 1998, pages 984-994. 31, 32, 65, 66
2) Heath, C Andrew and Roesler, R Jeffery (1999). Shrinkage and Thermal Cracking of Fast Setting Hydraulic Cement Concrete Pavements in Palmdale, *California*. *Preliminary report*, California Department of Transportation, December 1999. 31, 36, 37, 128
3) Zachary, C. Grasley, and Lange, David A. (2002). Modeling Drying Shrinkage Stress Gradients in Concrete. *Journal of Testing and Evaluation*, Vol. 26, No. 2, September 2002. 31
4) Levy, C. (2010), Numerical Investigation of the Effects of Shrinkage and Thermal Loading on the Behaviour of Misaligned Dowels in Jointed Concrete Pavement" *Thesis on Master of Applied Science in Civil Engineering*, 2010, University of Waterloo, Waterloo, Ontario, Canada
5) American Concrete Institute (2008). Prediction of Creep, Shrinkage, and Temperature Effects in Concrete Structures. *ACI 209R-92* (Re-approved 2008).